Supporting Information

Inorganometallic Allenes [(Mn(η⁵-C₅H₅)(CO)₂)₂(μ-E)] (E = Si – Pb): Bis Allylic Anionic Delocalisation Similar to Organometallic Allene but Differential σ-Donation and π-Backdonation

Parameswaran Parvathy and Pattiyil Parameswaran
Department of Chemistry
National Institute of Technology Calicut, Kerala, India-673601
param@nitc.ac.in

Table of Contents

Figure S1:Optimised geometries of heavy allenes a) **1E** and b) **1E$_{CH2}$** (E = Si-Pb) at BP86/def2-SVP level of theory; Given below is the pyramidalization angle (θ_E = 360-sum of angles around E) at the terminal E atom for **1E**.
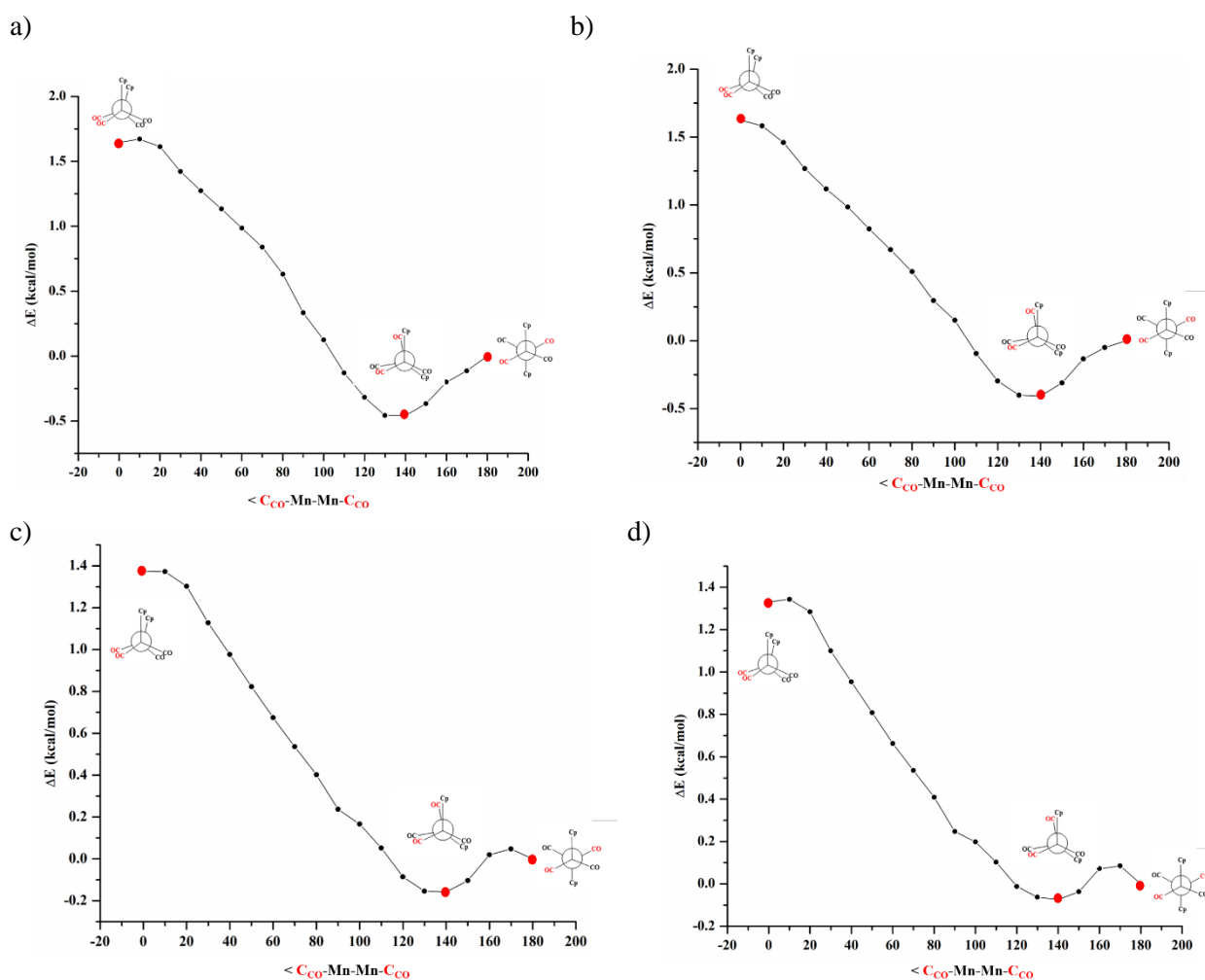
Figure S2: Rigid potential energy scan of **2Si** (a), **2Ge** (b), **2Sn** (c) and **2Pb** (d) by changing the C$_{CO}$-Mn-Mn-C$_{CO}$ dihedral angle by 10° from 180° to 0°. Selected points are highlighted in red.
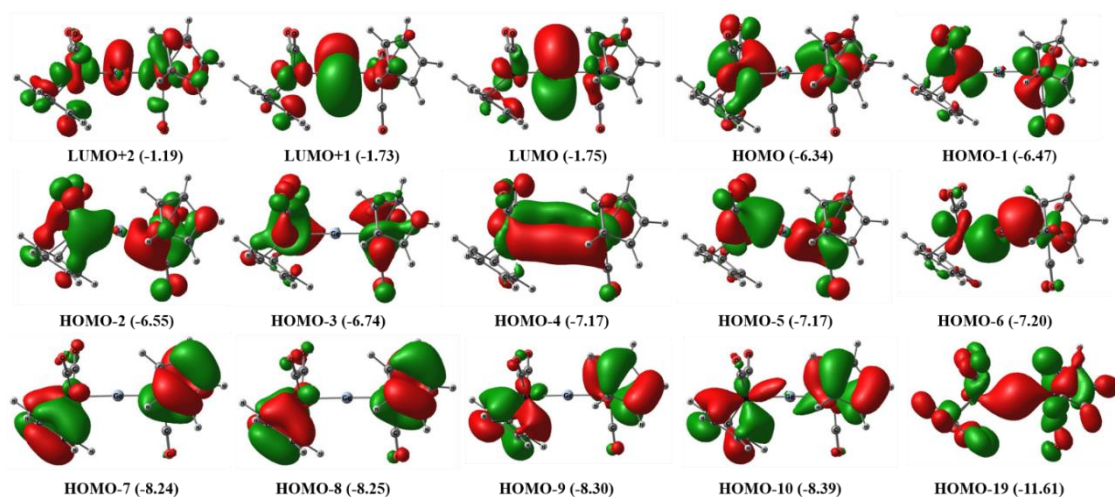
Figure S3: Selected frontier MOs of **2Ge** at M06/def2-TZVPP//BP86/def2-SVP level of theory; Eigen values given in eV in parentheses; Isosurface value 0.03
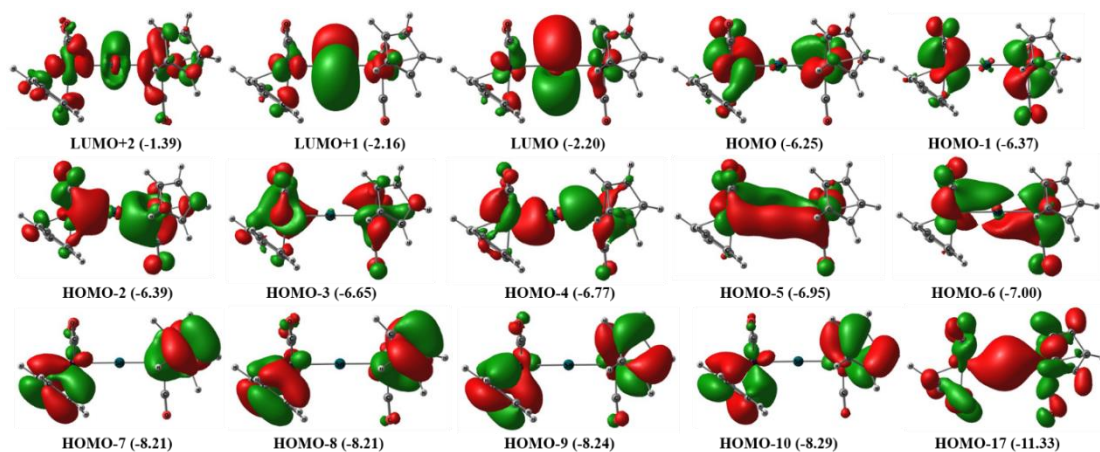
Figure S4: Selected frontier MOs of **2Sn** at M06/def2-TZVPP//BP86/def2-SVP level of theory; Eigen values given in eV in parentheses; Isosurface value 0.03
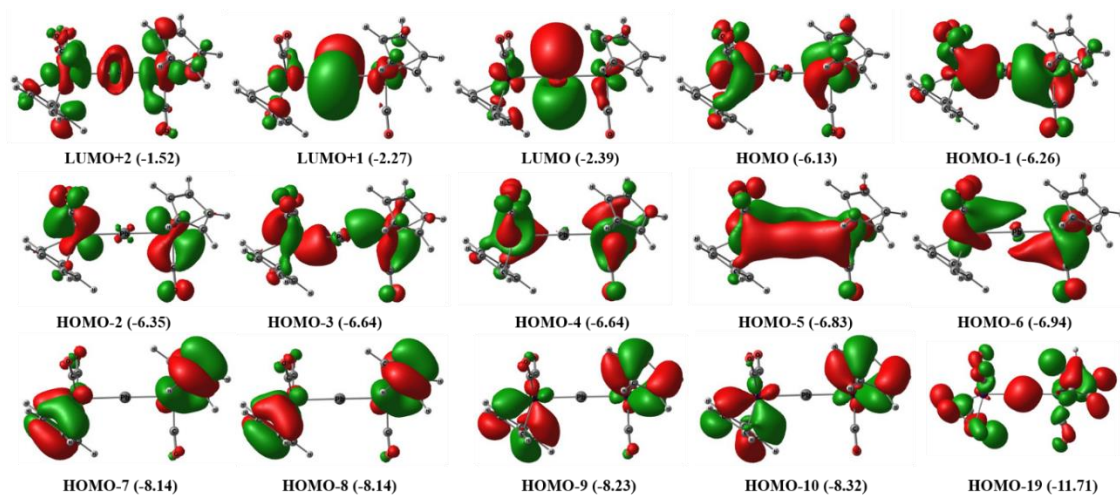
Figure S5: Selected frontier MOs of **2Pb** at M06/def2-TZVPP//BP86/def2-SVP level of theory; Eigen values given in eV in parentheses; Isosurface value 0.03

Table S1: Bond orbital occupancy (BO) from the NBO analysis of **1E** at M06/def2-TZVPP//BP86/def2-SVP level of theory.

| Compound	Bond	BO
2Si	Si-Mn1	1.84 (28.78% Si; 71.22% Mn)
		1.67 (95.55% Mn; 4.45% Si)
	Mn2-C1	1.95 (45.30% Mn; 54.70% C)
	Mn2-C2	1.95 (46.16% Mn; 53.84% C)
	C1-O1	2.00 (25.54% C; 74.46% O)
		1.99 (25.48% C; 74.52% O)
		1.99 (27.11% C; 72.89% O)
	LP(1) Mn1	1.61 (97.52% d)
	LP(2) Mn1	1.43 (73.46% d)
	LP(1) Mn2	1.61 (97.52% d)
	LP(2) Mn2	1.43 (73.46% d)
2Ge	Ge-Mn1	1.86 (34.27% Ge; 65.73% Mn)
		1.70 (6.40% Ge; 93.60% Mn)
	Mn2-C1	1.96 (44.56% Mn; 55.44% C)
	Mn2-C2	1.96 (45.01% Mn; 54.99% C)
	C1-O1	1.99 (27.62% C; 72.38% O)
		2.00 (23.46% C; 76.54% O)
		1.99 (26.70% C; 73.30% O)
	LP(1) Mn1	1.61 (97.78% d)
	LP(2) Mn1	1.44 (74.92% d)
	LP(1) Mn2	1.61 (97.78% d)
	LP(2) Mn2	1.44 (74.92% d)
2Sn	Sn-Mn1	1.83 (33.09% Sn; 66.91% Mn)
		1.70 (5.67% Sn; 94.33% Mn)
	Mn2-C1	1.96 (43.59% Mn; 56.41% C)
	Mn2-C2	1.96 (44.02% Mn; 55.98% C)
	C1-O1	1.99 (26.81% C; 73.19% O)
		2.00 (23.12% C; 76.88% O)
		1.99 (27.84% C; 72.16% O)
	LP(1) Mn1	1.60 (97.42% d)
	LP(2) Mn1	1.44 (74.80% d)
	LP(1) Mn2	1.60 (97.42% d)
	LP(2) Mn2	1.44 (74.80% d)
2Pb	Pb-Mn1	1.79 (37.80% Pb; 62.20% Mn)
		1.69 (3.92% Pb; 96.08% Mn)
	Mn2-C1	1.96 (43.22% Mn; 56.78% C)
	Mn2-C2	1.96 (43.58% Mn; 56.42% C)
	C1-O1	1.99 (27.16% C; 72.84% O)
		2.00 (23.27% C; 76.73% O)
		1.99 (27.37% C; 72.63% O)
	LP(1) Mn1	1.60 (97.34% d)
	LP(2) Mn1	1.46 (77.16% d)
	LP(1) Mn2	1.60 (97.34% d)
	LP(2) Mn2	1.46 (77.16% d)
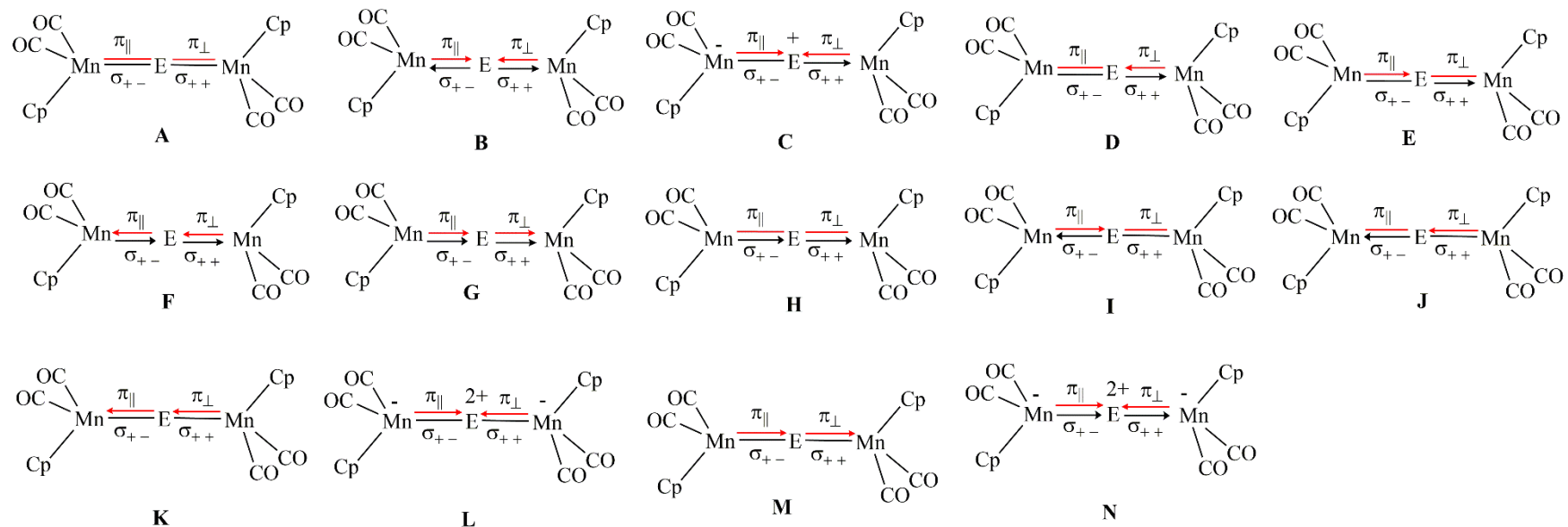
Scheme S1: Various bonding possibilities considered for the EDA-NOCV analysis of **2E** (E = C – Pb) at BP86/TZ2P level of theory; **2E** is fragmented in to E and (MnCp(CO)$_2$)$_2$; Straight lines depict electron sharing interactions, arrows depict donor-acceptor interactions; Red lines represent π-skeleton and black lines represent σ-skeleton; Bonding possibilities in the squares have the lowest ΔE$_{orb}$ values and are considered for detailed analysis.

Table S2: Results of EDA-NOCV analysis carried out for bonding possibilities A-M for compound **2E** at BP86/TZ2P level of theory;

Compound	Possibility	ΔE_{int}	ΔE_{elect}	ΔE_{Pauli}	ΔE_{orb}	ΔE_{disp}
2C	**A**	-344.56	-282.32	314.28	-369.60	-6.92
	B	-264.96	-457.08	512.19	-313.15	-6.92
	C	-453.74	-239.97	297.95	-504.79	-6.92
	D	-255.25	-286.28	397.54	-359.58	-6.92
	E	-252.24	-303.29	420.48	-362.51	-6.92
	F	-367.28	-67.45	176.83	-469.74	-6.92
	G	-362.08	-71.23	147.80	-431.72	-6.92
	H	-303.56	-134.53	286.13	-448.24	-6.92
	I	-403.28	-521.89	516.52	-390.98	-6.92
	J	-406.77	-528.99	543.69	-414.54	-6.92
	K	-454.23	-288.97	335.72	-494.05	-6.92
	L	-1185.04	-473.46	160.83	-865.48	-6.92
	M	-654.40	-276.14	322.08	-693.41	-6.92
	N	-1106.13	-274.99	95.24	-919.47	-6.92
2Si	**A**	-295.69	-295.06	327.48	-313.85	-14.26
	B	-204.28	-436.40	482.02	-235.64	-14.26
	C	-321.06	-260.04	226.55	-273.30	-14.26
	D	-202.14	-269.53	334.58	-252.93	-14.26
	E	-198.02	-263.30	319.53	-239.99	-14.26
	F	-285.13	-91.31	160.89	-340.46	-14.26
	G[a]					
	H	-238.93	-85.62	154.60	-293.66	-14.26
	I[a]					
	J	-337.80	-500.67	515.07	-337.94	-14.26
	K	-376.44	-307.37	342.00	-396.81	-14.26
	L	-874.94	-548.47	192.09	-504.30	-14.26
	M[a]					
	N	-762.91	-358.21	65.05	-455.49	-14.26
2Ge	**A**	-314.40	-292.06	309.12	-317.25	-14.21
	B	-189.24	-386.57	417.10	-205.57	-14.21
	C	-301.84	-242.60	190.97	-236.01	-14.21
	D	-188.57	-237.15	281.50	-218.72	-14.21
	E	-182.94	-234.46	273.55	-207.83	-14.21
	F	-269.54	-76.40	128.29	-307.23	-14.21
	G[a]					
	H	-223.01	-72.48	119.81	-256.14	-14.21
	I	-349.66	-470.17	460.14	-325.43	-14.21
	J	-355.93	-469.96	466.79	-338.56	-14.21
	K	-393.34	-304.30	320.94	-395.78	-14.21
	L	-884.44	-561.97	192.18	-500.44	-14.21
	M[a]					
	N	-729.18	-359.84	50.59	-405.72	-14.21
2Sn	**A**	-284.19	-279.11	293.69	-282.74	-16.03

	B	-169.47	-356.97	385.25	-181.73	-16.03
	C	-268.59	-236.59	176.68	-192.65	-16.03
	D	-170.01	-217.21	253.07	-189.84	-16.03
	E	-163.68	-215.00	246.38	-179.02	-16.03
	F	-245.83	-80.25	119.91	-269.44	-16.03
	G	-233.08	-78.17	104.34	-243.22	-16.03
	H	-201.45	-77.64	110.78	-218.56	-16.03
	I	-314.50	-439.07	433.58	-292.98	-16.03
	J	-321.31	-437.18	436.90	-304.99	-16.03
	K	-356.50	-286.55	301.20	-355.13	-16.03
	L	-796.05	-561.00	196.09	-415.10	-16.03
	M[a]					
	N	-656.01	-377.05	55.53	-318.45	-16.03
2Pb	**A**	-318.53	-270.06	280.19	-311.91	-16.75
	B	-156.73	-336.75	364.25	-167.48	-16.75
	C	-247.85	-224.28	166.75	-173.56	-16.75
	D	-157.93	-202.50	236.11	-174.79	-16.75
	E	-152.53	-197.50	225.09	-163.37	-16.75
	F	-232.06	-74.96	112.96	-253.31	-16.75
	G[a]					
	H	-190.02	-68.10	96.32	-201.49	-16.75
	I	-346.65	-420.99	413.47	-322.38	-16.75
	J	-352.46	-420.75	419.34	-334.30	-16.75
	K	-388.03	-275.43	289.17	-385.02	-16.75
	L	-810.43	-354.92	201.47	-438.77	-16.75
	M[a]					
	N	-619.44	-374.46	60.57	-288.80	-16.75

[a] Calculations did not converge to correct electronic states while preparing the fragments for the EDA-NOCV calculations; These possibilities are found to have high negative values of ΔE_{orb} for **2C**.

Table S3: Detailed results of EDA-NOCV analysis for bonding possibilities D and E of compounds **2E** (E = Si-Pb) at BP86/TZ2P level of theory.

	2Si		2Ge		2Sn		2Pb	
	D	E	D	E	D	E	D	E
ΔE_{int}	-202.14	-198.02	-188.57	-182.94	-170.01	-163.68	-157.93	-152.53
ΔE_{elect}[a]	-269.53 (51.59%)	-263.30 (52.32%)	-237.15 (52.02%)	-234.46 (53.01%)	-217.21 (53.36%)	-215.00 (54.55%)	-202.50 (53.67%)	-197.50 (54.73%)
ΔE_{Pauli}	334.58	319.53	281.5	273.55	253.07	246.38	236.11	225.09
ΔE_{orb}[a]	-252.93 (48.41%)	-239.99 (47.68%)	-218.72 (47.98%)	-207.83 (46.99%)	-189.84 (46.64%)	-179.02 (45.43%)	-174.79 (46.33%)	-163.37 (45.27%)
$\Delta E_{\sigma++}$[b]	-29.40 (11.62%)	-30.43 (12.68%)	-23.58 (10.78%)	-22.33 (10.74%)	-20.61 (10.86%)	-20.02 (11.18%)	-14.29 (8.17%)	-14.07 (8.61%)
$\Delta E_{\sigma+-}$[b]	-84.56 (33.43%)	-85.15 (35.48%)	-79.01 (36.12%)	-79.30 (38.16%)	-70.08 (36.92%)	-70.24 (39.23%)	-70.19 (40.16%)	-70.57 (43.19%)
$\Delta E_{\pi\perp}$[b]	-45.71 (18.07%)	-68.64 (28.60%)	-35.22 (16.10%)	-62.23 (29.94%)	-26.14 (13.77%)	-54.63 (30.52%)	-23.39 (13.38%)	-50.97 (31.20%)
$\Delta E_{\pi\|}$[b]	-72.55 (28.69%)	-35.61 (14.84%)	-68.95 (31.52%)	-32.55 (15.66%)	-62.91 (33.14%)	-24.54 (13.71%)	-58.66 (33.56%)	-20.00 (12.24%)
ΔE_{rest}[c]	-20.77 (8.21%)	-20.21 (8.42%)	-12.02 (5.50%)	-11.47 (5.52%)	-10.13 (5.33%)	-9.63 (5.38%)	-8.31 (4.76%)	-7.82 (4.79%)
ΔE_{prep}	16.75	12.63	18.76	13.13	18.61	12.28	16.94	11.54
$-D_e$	-185.39	-185.39	-169.81	-169.81	-151.4	-151.40	-140.99	-140.99

[a] values in parentheses give the percentage contribution to attractive interactions $\Delta E_{orb}+\Delta E_{elect}$; [b] values in parentheses give the percentage contribution to the orbital interaction, ΔE_{orb}; [c] $\Delta E_{rest} = \Delta E_{orb} - (\Delta E_{\sigma++} + \Delta E_{\sigma+} + \Delta E_{\pi\perp} + \Delta E_{\pi\|})$.

Table S4: Detailed results of EDA-NOCV analysis for bonding possibility C of compounds **2E** (E = Si-Pb) at BP86/TZ2P level of theory;

|	**2Si**	**2Ge**	**2Sn**	**2Pb**
ΔE_{int}	-321.06	-301.84	-268.59	-247.85
ΔE_{elect}[a]	-260.04 (48.76%)	-242.6 (50.69%)	-236.59 (55.12%)	-224.28 (56.37%)
ΔE_{Pauli}	226.55	190.97	176.68	166.75
ΔE_{orb}[a]	-273.30 (51.24%)	-236.01 (49.31%)	-192.65 (44.88%)	-173.56 (43.63%)
$\Delta E_{\sigma++}$[b]	-29.52 (10.80%)	-21.04 (8.91%)	-18.30 (9.50%)	-13.21 (7.61%)
$\Delta E_{\sigma+-}$[b]	-91.64 (33.53%)	-86.69 (36.73%)	-75.44 (39.16%)	-74.77 (43.08%)
$\Delta E_{\pi\perp}$[b]	-58.99 (21.58%)	-51.59 (21.86%)	-38.82 (20.15%)	-35.87 (20.67%)
$\Delta E_{\pi\parallel}$[b]	-50.74 (18.57%)	-46.74 (19.80%)	-35.39 (18.37%)	-29.37 (16.92%)
ΔE_{rest}[c]	-42.41 (15.52%)	-29.93 (12.68%)	-24.65 (12.80%)	-20.32 (11.71%)
ΔE_{prep}	135.67	132.03	117.19	106.86
-D$_e$	-185.39	-169.81	-151.4	-140.99

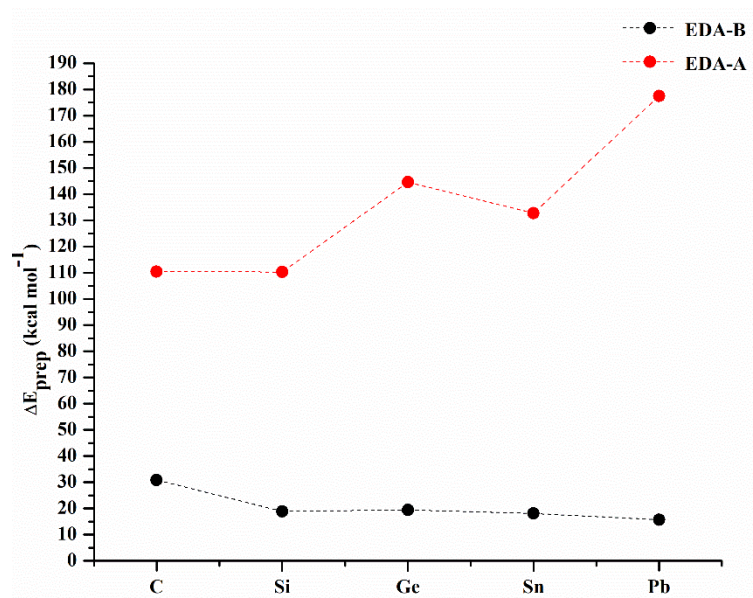[a] values in parentheses give the percentage contribution to attractive interactions $\Delta E_{orb}+\Delta E_{elect}$; [b] values in parentheses give the percentage contribution to the orbital interaction, ΔE_{orb}; [c] $\Delta E_{rest} = \Delta E_{orb} - (\Delta E_{\sigma++} + \Delta E_{\sigma+} + \Delta E_{\pi\perp} + \Delta E_{\pi\parallel})$.
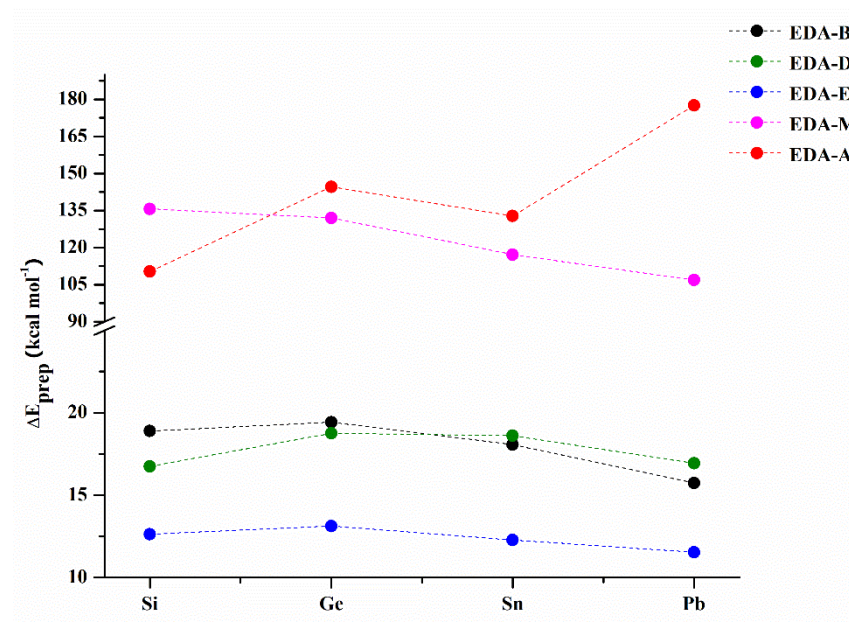
Figure S6: a) Plot of ΔE_{prep} for bonding possibility A and B in compounds **2E** (E =C-Pb) and b) a) plot of ΔE_{prep} for bonding possibility B, D, E, M and A in compounds **2E** (E =Si-Pb) at BP86/TZ2Plevel of theory.
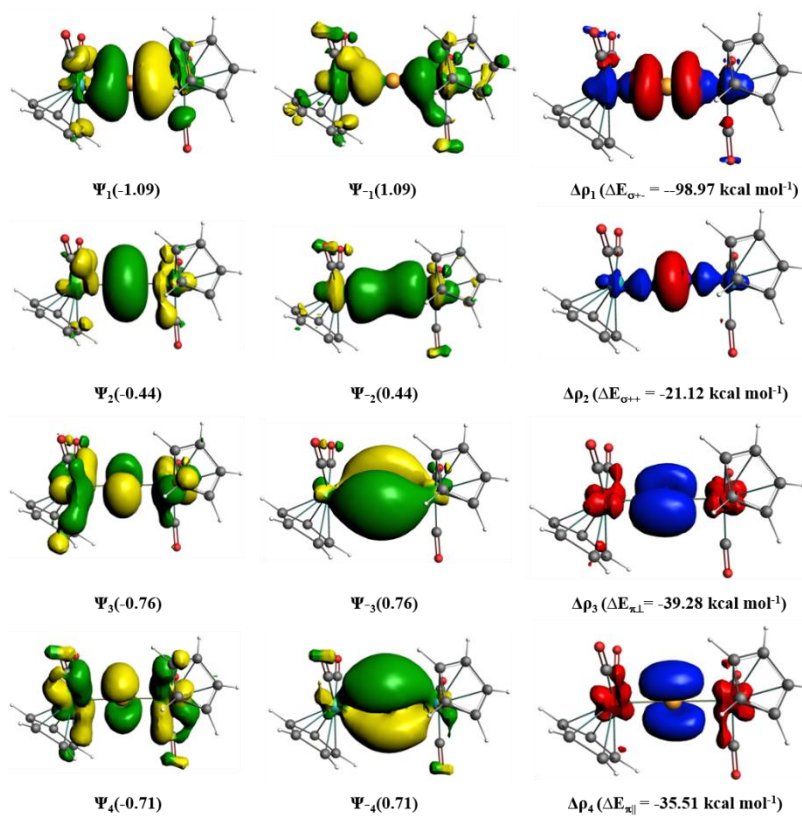
Note: Before looking into the detailed energy decomposition data for bonding possibilities D, E and M, we shall look at the trend in the ΔE_{prep} for these bonding possibilities in **2E** (E = Si-Pb, Figure S6). Bonding possibility E has the lowest values of ΔE_{prep} for all the compounds. Generalising, bonding possibilities where the central tetrel atom is present in its ground ^3P state is found to have low values of ΔE_{prep}, except in **2Sn** and **2Pb** where the preparatory energy for possibility D is higher than that for the dative possibility B. The preparatory energy associated with the charge separated bonding possibility C is high for **2Si** and **2Ge** and decreases, although only marginally, for **2Sn** and **2Pb**. Thus, the energy associated for preparing the fragments to the electronic state in bonding possibility C, where the tetrel atom is positively charged and the $(MnCp(CO)_2)_2$ fragments are negatively charged, is very demanding.

The detailed energy decomposition data for the bonding possibilities D and E is summarised in Table S3, and the plots of the deformation density with the associated NOCV orbitals are given in the Figure S8-Figure S11. The bonding possibility D and E, where the tetrel atom is present in its ground ^3P state have low values of ΔE_{orb} for **2Si-2Pb**. The magnitude of ΔE_{elect} and ΔE_{orb} decreases as the group-14 atom is changed from C to Pb for both bonding possibilities D and E. However, unlike bonding possibility B where the percentage contribution of ΔE_{elect} and ΔE_{orb} towards total ΔE_{orb} increases and decreases respectively, here the percentage contribution of ΔE_{elect} and ΔE_{orb} remains comparable throughout the group. In both possibilities, the doubly occupied ns-orbital is involved in the donor-acceptor type σ_{++} interaction, while the singly occupied np_z-orbital is involved in an electron-sharing σ_{+-} interaction with the singly occupied anti-bonding combination of σ-group orbitals on the TM fragment. Similar to the dative possibility B, the energy associated with the former interaction contributes least to the overall ΔE_{orb} and the magnitude decreases as the tetrel atom is changed from C (-29.40 kcal mol^{-1} for D; -30.43 kcal mol^{-1} for E) to Pb (-14.29 kcal mol^{-1} for D; -14.07 kcal mol^{-1} for E). The np_z orbital is still responsible for the maximum contribution to the overall orbital stabilisation, however, the magnitude of this stabilisation energy is lesser when the σ_{+-} interaction has an electron-sharing nature as compared to the dative nature in bonding possibility B. The bonding possibilities D and E differ in the nature of the π-skeleton, where the former features an electron-sharing $\pi_{\parallel}$ bond (^3P; $ns^2 np_z^1 np_x^1 np_y^0$) and latter features an electron-sharing $\pi_{\perp}$ bond (^3P; $ns^2 np_z^1 np_x^0 np_y^1$). The magnitude of stabilisation energy associated with these π-bonds are found to be higher when the π-interaction has an electron-sharing nature viz. $\Delta E_{\pi\parallel}$ and $\Delta E_{\pi\perp}$ in **2Si** for possibility D are -72.55 kcal mol^{-1} and -45.71 kcal mol^{-1} respectively, and the same for possibility E are -35.61 kcal mol^{-1} and -65.61 kcal mol^{-1} respectively. The heavier analogs show the same trend. Moreover, the energy associated with an electron-sharing π-interaction is higher in magnitude that the energy for the corresponding donor-acceptor π-interaction in bonding possibility B.

The bonding possibility C has comparable ΔE_{orb} values for **2Sn** and **2Pb**, and the detailed energy decomposition data is summarised in Table S4. Note that the destabilisation associated with the Pauli's repulsion ΔE_{Pauli} is notably low for bonding possibility C (176.68 kcal mol^{-1} for **2Sn** and 166.75 kcal mol^{-1} for **2Pb**) in comparison to the same for bonding possibilities A, B, D and E for **2Sn** and **2Pb**. Also, the energy contribution from the electrostatic interaction (55.12% for **2Sn** and 56.37% for **2Pb**) is dominant over the orbital interaction for both compounds. This is in accordance with the charge-separated nature of the fragments involved. The plots of the deformation density and the associated NOCV orbitals are given in the Figure S13. Similar to the previously discussed bonding scenarios, the σ_{+-} interaction has the highest contribution towards ΔE_{orb} viz. -75.44 kcal mol^{-1} for **2Sn** (39.61%) and -74.77 kcal mol^{-1} for **2Pb** (49.08%). The two π-type back-donations from the $(MnCp(CO)_2)_2$ group viz. $\pi_{\perp}$ and $\pi_{\parallel}$ contribute almost equally to the ΔE_{orb}. The associated $\Delta E_{\pi\perp}$ and $\Delta E_{\pi\parallel}$ for **2Sn** are -38.82 kcal mol^{-1} and 35.39 kcal mol^{-1}, while that for **2Pb** are 35.87 kcal mol^{-1} and 29.37 kcal mol^{-1}respectively.

The σ++ interaction contributes the least to the ΔEorb, consistent with the trend for the previously discussed possibilities.

a)

$\Psi_1(-1.09)$ $\Psi_{-1}(1.09)$ $\Delta\rho_1$ ($\Delta E_{\sigma+-}$ = −98.97 kcal mol^{-1})

$\Psi_2(-0.44)$ $\Psi_{-2}(0.44)$ $\Delta\rho_2$ ($\Delta E_{\sigma++}$ = -21.12 kcal mol^{-1})

$\Psi_3(-0.76)$ $\Psi_{-3}(0.76)$ $\Delta\rho_3$ ($\Delta E_{\pi\perp}$ = -39.28 kcal mol^{-1})

$\Psi_4(-0.71)$ $\Psi_{-4}(0.71)$ $\Delta\rho_4$ ($\Delta E_{\pi\parallel}$ = -35.51 kcal mol^{-1})

b)

$\Psi_1(-1.10)$ $\Psi_{-1}(1.10)$ $\Delta\rho_1$ ($\Delta E_{\sigma+-}$ = −95.86 kcal mol^{-1})

$\Psi_2(-0.43)$ $\Psi_{-2}(0.43)$ $\Delta\rho_2$ ($\Delta E_{\sigma++}$ = -19.00 kcal mol^{-1})

$\Psi_3(-0.74)$ $\Psi_{-3}(0.74)$ $\Delta\rho_3$ ($\Delta E_{\pi\perp}$ = -30.38 kcal mol^{-1})

$\Psi_4(-0.69)$ $\Psi_{-4}(0.69)$ $\Delta\rho_4$ ($\Delta E_{\pi\parallel}$ = -27.22 kcal mol^{-1})

c)

$\Psi_1(-1.12)$ $\Psi_{-1}(1.12)$ $\Delta\rho_1\ (\Delta E_{\sigma+-} = -95.97\ \text{kcal mol}^{-1})$

$\Psi_2(-0.32)$ $\Psi_{-2}(0.32)$ $\Delta\rho_2\ (\Delta E_{\sigma++} = -13.64\ \text{kcal mol}^{-1})$

$\Psi_3(-0.73)$ $\Psi_{-3}(0.73)$ $\Delta\rho_3\ (\Delta E_{\pi\perp} = -27.78\ \text{kcal mol}^{-1})$

$\Psi_4(-0.64)$ $\Psi_{-4}(0.64)$ $\Delta\rho_4\ (\Delta E_{\pi\parallel} = -22.68\ \text{kcal mol}^{-1})$
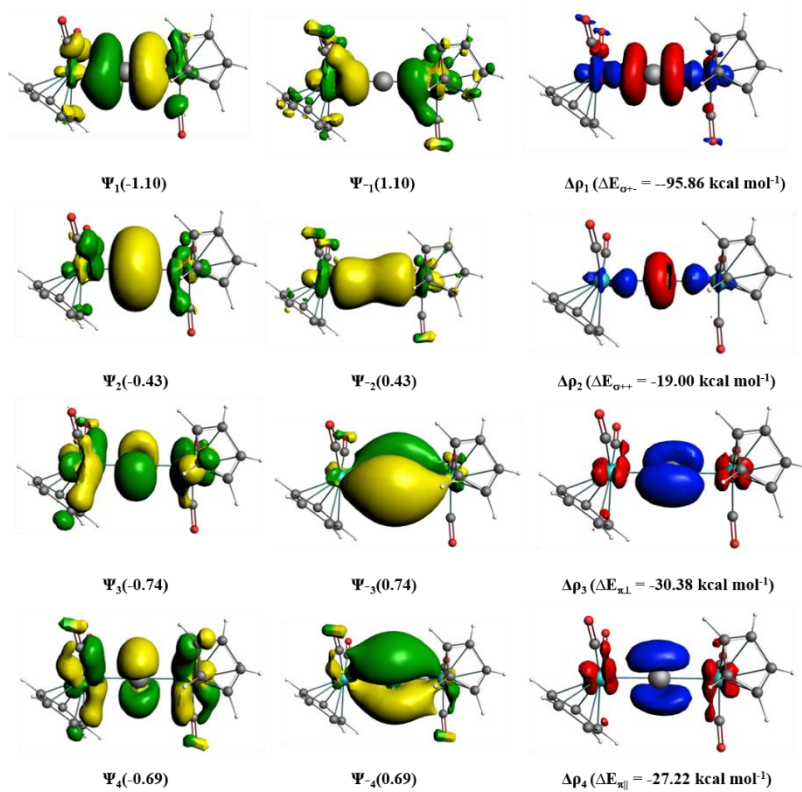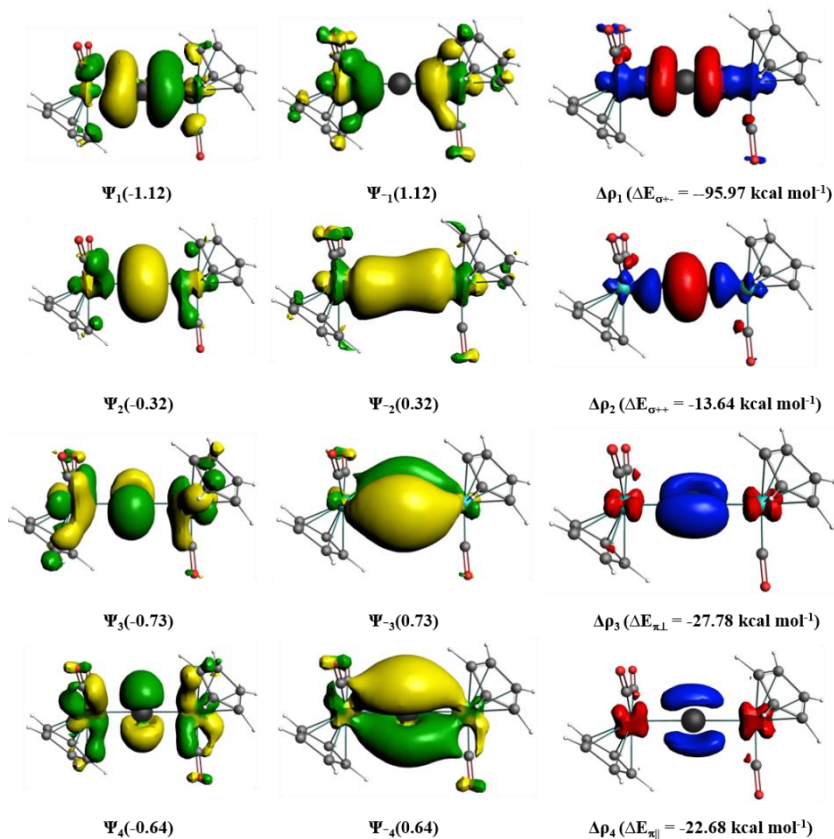
Figure S7: Plots of important NOCV pair of orbitals Ψ_{-n}/Ψ_n of dative bonding possibility B in **2Ge** (a), **2Sn** (b), **2Pb** (c) with their eigen values in parenthesis, the deformation densities $\Delta\rho_n$ and the corresponding orbital stabilization energies ΔE (kcal mol^{-1}) at the BP86/TZ2P level of theory. The direction of the charge flow in the deformation density plot $\Delta\rho_n$ is from red→blue. The isosurface values for NOCV orbitals and deformation densities are 0.03 and 0.003 respectively.

a)

$\Psi_1(-0.47)$	$\Psi_{-1}(0.47)$	$\Delta\rho_1 (\Delta E_{\sigma+-} = -84.56$ kcal mol$^{-1})$
$\Psi_2(-0.25)$	$\Psi_{-2}(0.25)$	$\Delta\rho_2 (\Delta E_{\sigma++} = -29.40$ kcal mol$^{-1})$
$\Psi_3(-0.44)$	$\Psi_{-3}(0.44)$	$\Delta\rho_3 (\Delta E_{\pi\perp} = -45.71$ kcal mol$^{-1})$
$\Psi_4(-0.36)$	$\Psi_{-4}(0.36)$	$\Delta\rho_4 (\Delta E_{\pi\parallel} = -72.55$ kcal mol$^{-1})$

b)

$\Psi_1(-0.47)$	$\Psi_{-1}(0.47)$	$\Delta\rho_1 (\Delta E_{\sigma+-} = -85.15$ kcal mol$^{-1})$
$\Psi_2(-0.25)$	$\Psi_{-2}(0.25)$	$\Delta\rho_2 (\Delta E_{\sigma++} = -30.43$ kcal mol$^{-1})$
$\Psi_3(-0.44)$	$\Psi_{-3}(0.44)$	$\Delta\rho_3 (\Delta E_{\pi\perp} = -68.64$ kcal mol$^{-1})$
$\Psi_4(-0.36)$	$\Psi_{-4}(0.36)$	$\Delta\rho_4 (\Delta E_{\pi\parallel} = -35.61$ kcal mol$^{-1})$
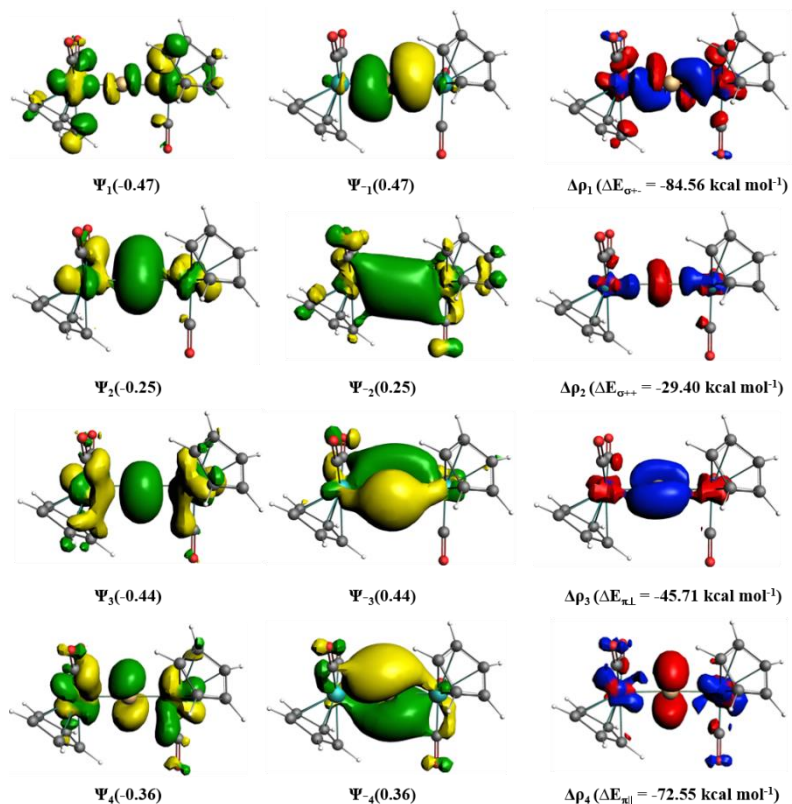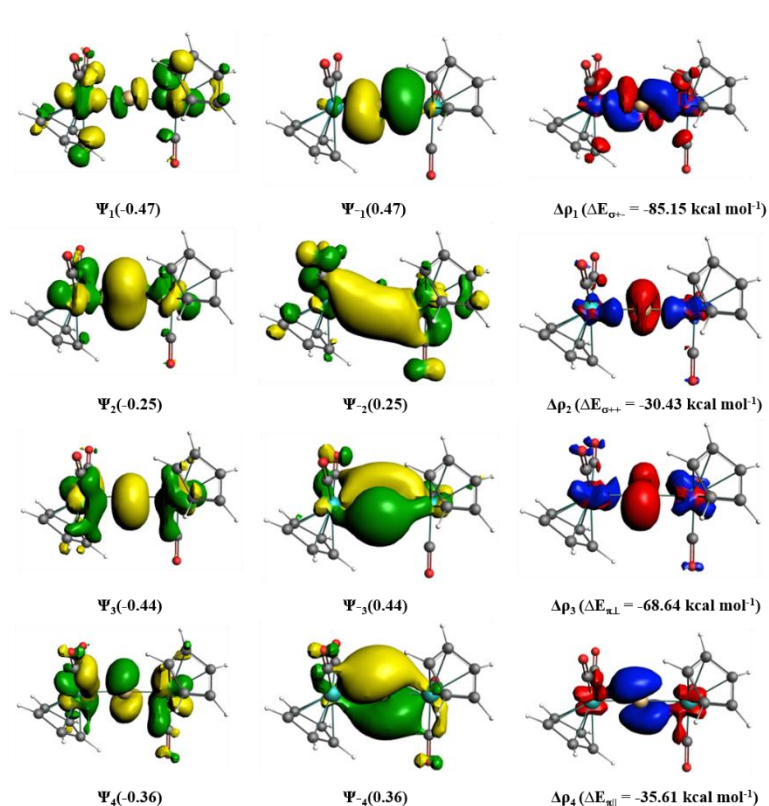
Figure S8: Plots of important alpha-NOCV pair of orbitals Ψ_{-n}/Ψ_n of bonding possibility D (a) and E (b) in **2Si** with their eigen values in parenthesis, the deformation densities $\Delta\rho_n$ and the corresponding orbital stabilization energies ΔE (kcal mol^{-1}) at the BP86/TZ2P level of theory. The direction of the charge flow in the deformation density plot $\Delta\rho_n$ is from red→blue. The isosurface values for NOCV orbitals and deformation densities are 0.03 and 0.003 respectively.

$\Psi_1(-0.46)$ $\Psi_{-1}(0.46)$ $\Delta\rho_1 (\Delta E_{\sigma+-} = --79.01 \text{ kcal mol}^{-1})$

$\Psi_1(-0.45)$ $\Psi_{-1}(0.45)$ $\Delta\rho_1 (\Delta E_{\sigma+-} = --79.30 \text{ kcal mol}^{-1})$

$\Psi_2(-0.24)$ $\Psi_{-2}(0.24)$ $\Delta\rho_2 (\Delta E_{\sigma++} = -23.58 \text{ kcal mol}^{-1})$

$\Psi_2(-0.26)$ $\Psi_{-2}(0.26)$ $\Delta\rho_2 (\Delta E_{\sigma++} = -22.33 \text{ kcal mol}^{-1})$

$\Psi_3(-0.39)$ $\Psi_{-3}(0.39)$ $\Delta\rho_3 (\Delta E_{\pi\perp} = -35.22 \text{ kcal mol}^{-1})$

$\Psi_3(-0.41)$ $\Psi_{-3}(0.41)$ $\Delta\rho_3 (\Delta E_{\pi\perp} = -62.23 \text{ kcal mol}^{-1})$

$\Psi_4(-0.37)$ $\Psi_{-4}(0.37)$ $\Delta\rho_4 (\Delta E_{\pi\parallel} = -68.95 \text{ kcal mol}^{-1})$

$\Psi_4(-0.36)$ $\Psi_{-4}(0.36)$ $\Delta\rho_4 (\Delta E_{\pi\parallel} = -32.55 \text{ kcal mol}^{-1})$

Figure S9: Plots of important alpha-NOCV pair of orbitals Ψ_{-n}/ Ψ_n of bonding possibility D (a) and E (b) in **2Ge** with their eigen values in parenthesis, the deformation densities $\Delta\rho_n$ and the corresponding orbital stabilization energies ΔE (kcal mol^{-1}) at the BP86/TZ2P level of theory. The direction of the charge flow in the deformation density plot $\Delta\rho_n$ is from red→blue. The isosurface values for NOCV orbitals and deformation densities are 0.03 and 0.003 respectively.

a)

$\Psi_1(-0.44)$ $\Psi_{-1}(0.44)$ $\Delta\rho_1$ ($\Delta E_{\sigma+-}$ = −20.61 kcal mol^{-1})

$\Psi_2(-0.25)$ $\Psi_{-2}(0.25)$ $\Delta\rho_2$ ($\Delta E_{\sigma++}$ = -70.08 kcal mol^{-1})

$\Psi_3(-0.38)$ $\Psi_{-3}(0.38)$ $\Delta\rho_3$ ($\Delta E_{\pi\perp}$ = -26.14 kcal mol^{-1})

$\Psi_4(-0.35)$ $\Psi_{-4}(0.35)$ $\Delta\rho_4$ ($\Delta E_{\pi\parallel}$ = -62.91 kcal mol^{-1})

b)

$\Psi_1(-0.43)$ $\Psi_{-1}(0.43)$ $\Delta\rho_1$ ($\Delta E_{\sigma+-}$ = −70.24 kcal mol^{-1})

$\Psi_2(-0.25)$ $\Psi_{-2}(0.25)$ $\Delta\rho_2$ ($\Delta E_{\sigma++}$ = -20.02 kcal mol^{-1})

$\Psi_3(-0.39)$ $\Psi_{-3}(0.39)$ $\Delta\rho_3$ ($\Delta E_{\pi\perp}$ = -54.63 kcal mol^{-1})

$\Psi_4(-0.35)$ $\Psi_{-4}(0.35)$ $\Delta\rho_4$ ($\Delta E_{\pi\parallel}$ = -24.54 kcal mol^{-1})

Figure S10: Plots of important alpha-NOCV pair of orbitals Ψ_{-n}/ Ψ_n of bonding possibility D (a) and E (b) in **2Sn** with their eigen values in parenthesis, the deformation densities $\Delta\rho_n$ and the corresponding orbital stabilization energies ΔE (kcal mol^{-1}) at the BP86/TZ2P level of theory. The direction of the charge flow in the deformation density plot $\Delta\rho_n$ is from red→blue. The isosurface values for NOCV orbitals and deformation densities are 0.03 and 0.003 respectively.
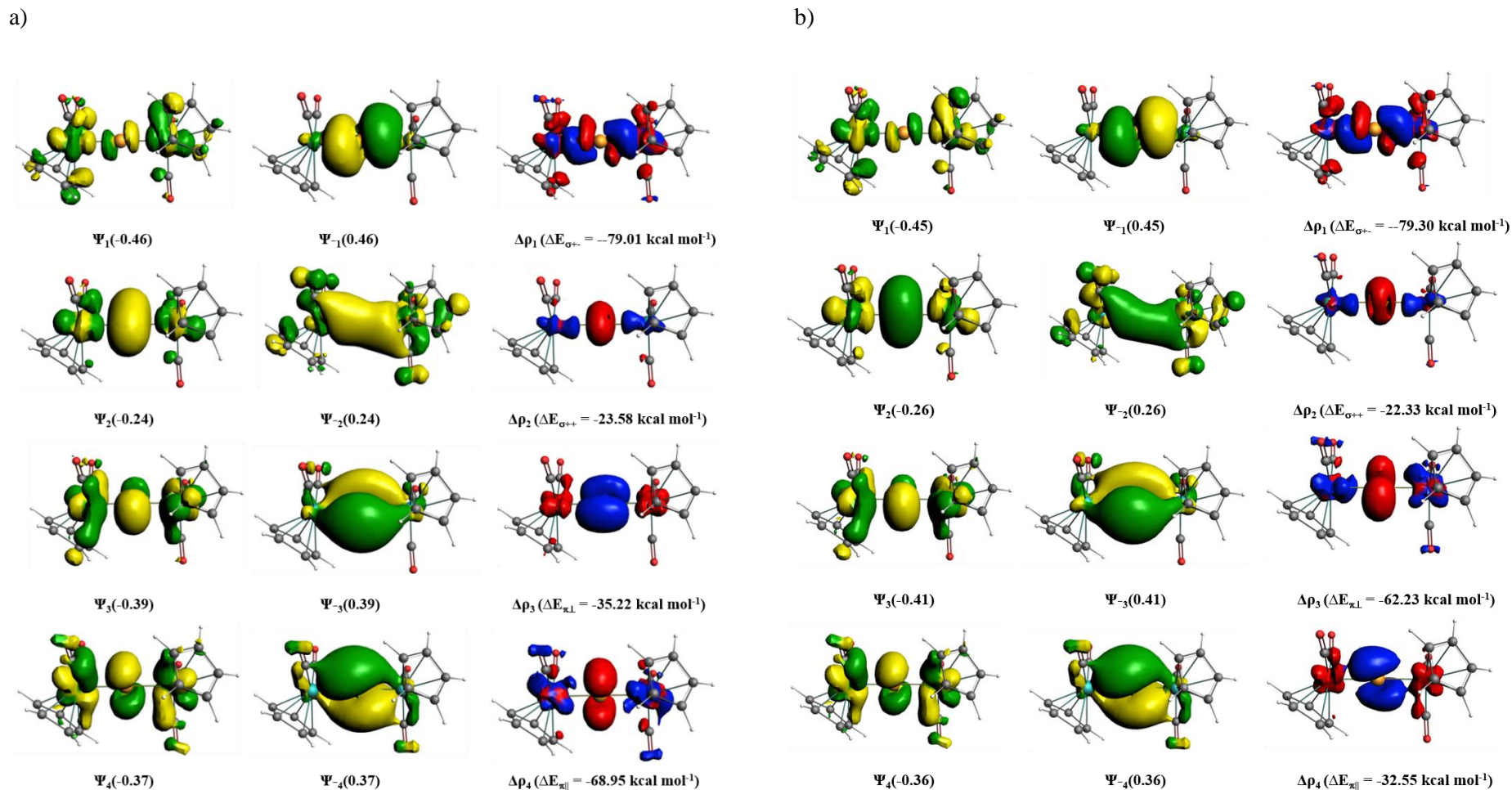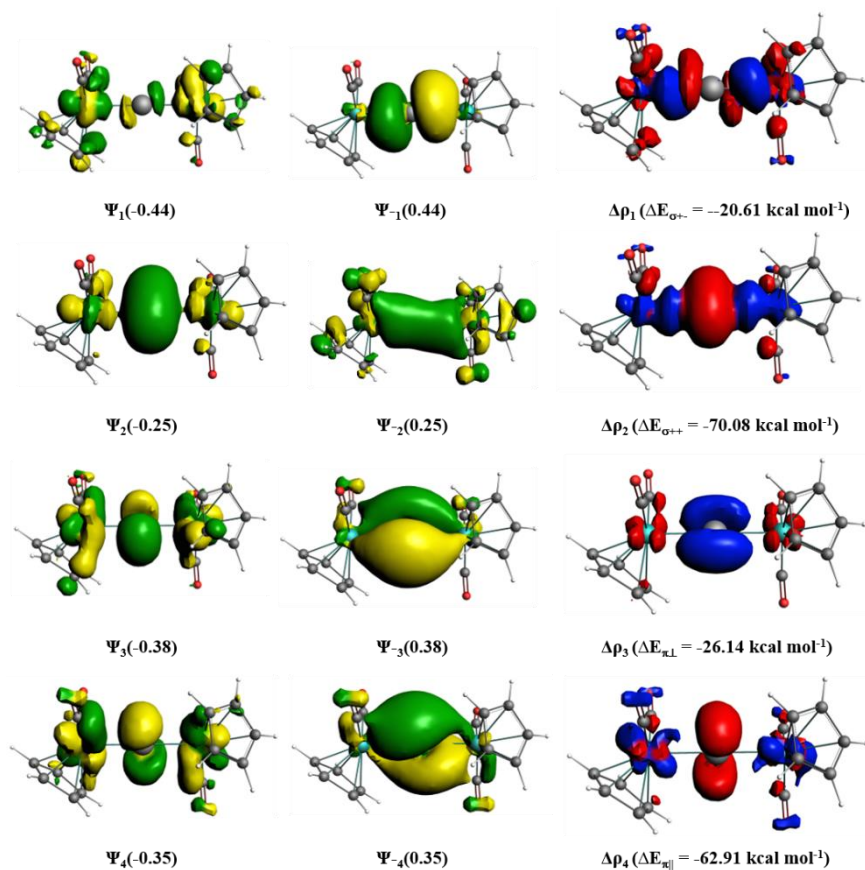
a)

$\Psi_1(-0.44)$ $\Psi_{-1}(0.44)$ $\Delta\rho_1$ ($\Delta E_{\sigma+-} = -70.19$ kcal mol^{-1})

$\Psi_2(-0.21)$ $\Psi_{-2}(0.21)$ $\Delta\rho_2$ ($\Delta E_{\sigma++} = -14.29$ kcal mol^{-1})

$\Psi_3(-0.37)$ $\Psi_{-3}(0.37)$ $\Delta\rho_3$ ($\Delta E_{\pi\perp} = -23.39$ kcal mol^{-1})

$\Psi_4(-0.33)$ $\Psi_{-4}(0.33)$ $\Delta\rho_4$ ($\Delta E_{\pi\parallel} = -58.66$ kcal mol^{-1})

b)

$\Psi_1(-0.43)$ $\Psi_{-1}(0.43)$ $\Delta\rho_1$ ($\Delta E_{\sigma+-} = -70.57$ kcal mol^{-1})

$\Psi_2(-0.21)$ $\Psi_{-2}(0.21)$ $\Delta\rho_2$ ($\Delta E_{\sigma++} = -14.07$ kcal mol^{-1})

$\Psi_3(-0.38)$ $\Psi_{-3}(0.38)$ $\Delta\rho_3$ ($\Delta E_{\pi\perp} = -50.97$ kcal mol^{-1})

$\Psi_4(-0.32)$ $\Psi_{-4}(0.32)$ $\Delta\rho_4$ ($\Delta E_{\pi\parallel} = -20.00$ kcal mol^{-1})
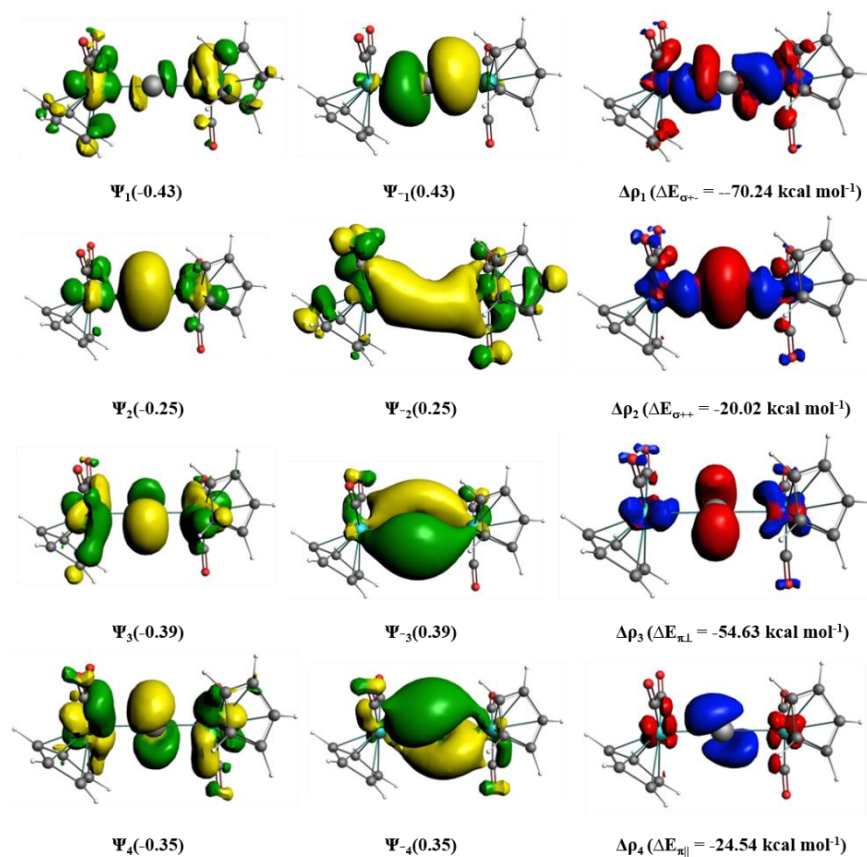
Figure S11: Plots of important alpha-NOCV pair of orbitals Ψ_{-n}/Ψ_n of bonding possibility D (a) and E (b) in **2Pb** with their eigen values in parenthesis, the deformation densities $\Delta\rho_n$ and the corresponding orbital stabilization energies ΔE (kcal mol^{-1}) at the BP86/TZ2P level of theory. The direction of the charge flow in the deformation density plot $\Delta\rho_n$ is from red→blue. The isosurface values for NOCV orbitals and deformation densities are 0.03 and 0.003 respectively.
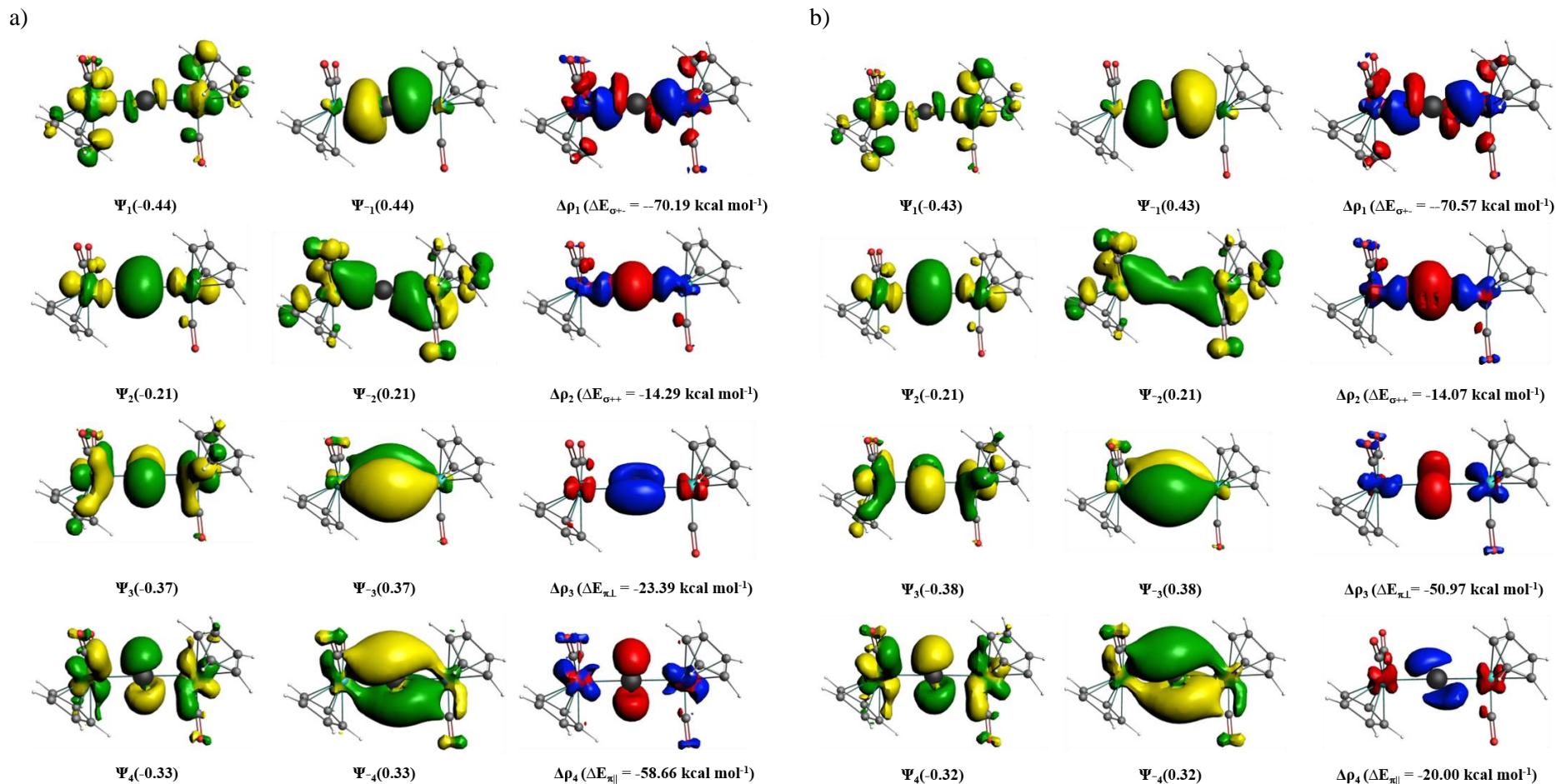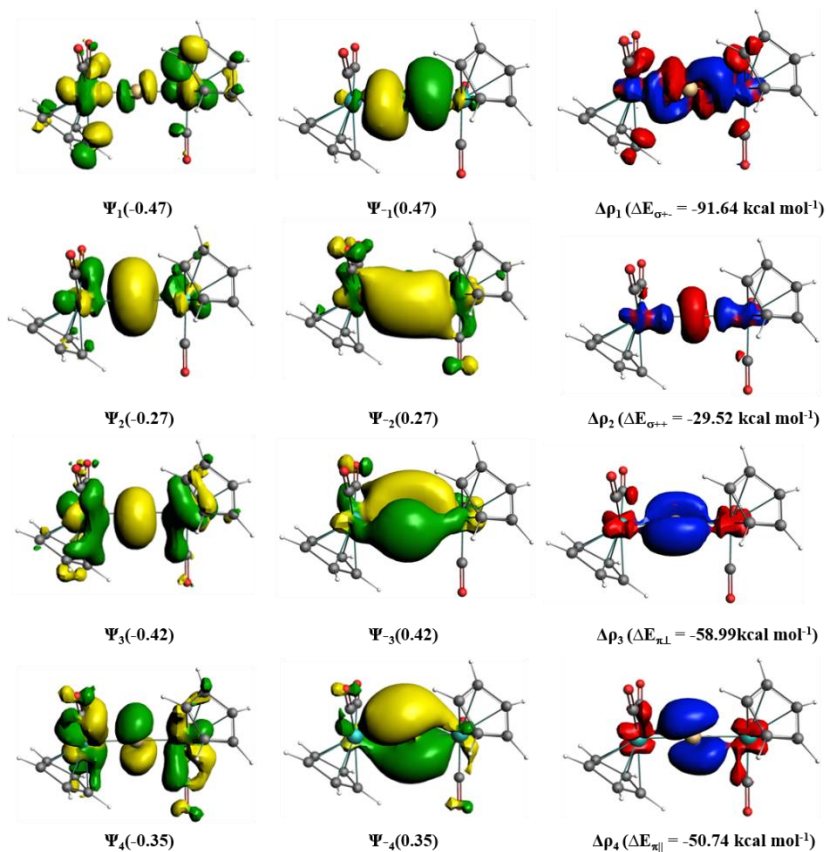
a)

Ψ_1(-0.47)	Ψ_{-1}(0.47)	$\Delta\rho_1$ ($\Delta E_{\sigma+-}$ = -91.64 kcal mol^{-1})
Ψ_2(-0.27)	Ψ_{-2}(0.27)	$\Delta\rho_2$ ($\Delta E_{\sigma++}$ = -29.52 kcal mol^{-1})
Ψ_3(-0.42)	Ψ_{-3}(0.42)	$\Delta\rho_3$ ($\Delta E_{\pi\perp}$ = -58.99 kcal mol^{-1})
Ψ_4(-0.35)	Ψ_{-4}(0.35)	$\Delta\rho_4$ ($\Delta E_{\pi\parallel}$ = -50.74 kcal mol^{-1})

b)

Ψ_1(-0.46)	Ψ_{-1}(0.46)	$\Delta\rho_1$ ($\Delta E_{\sigma+-}$ = -86.69 kcal mol^{-1})
Ψ_2(-0.25)	Ψ_{-2}(0.25)	$\Delta\rho_2$ ($\Delta E_{\sigma++}$ = -21.04 kcal mol^{-1})
Ψ_3(-0.38)	Ψ_{-3}(0.38)	$\Delta\rho_3$ ($\Delta E_{\pi\perp}$ = -51.59 kcal mol^{-1})
Ψ_4(-0.35)	Ψ_{-4}(0.35)	$\Delta\rho_4$ ($\Delta E_{\pi\parallel}$ = -46.74 kcal mol^{-1})

Figure S12: Plots of important alpha-NOCV pair of orbitals Ψ_{-n}/ Ψ_n of bonding possibility C in **2Si** (a) and **2Ge** (b) with their eigen values in parenthesis, the deformation densities $\Delta\rho_n$ and the corresponding orbital stabilization energies ΔE (kcal mol^{-1}) at the BP86/TZ2P level of theory. The direction of the charge flow in the deformation density plot $\Delta\rho_n$ is from red→blue. The isosurface values for NOCV orbitals and deformation densities are 0.03 and 0.003 respectively.
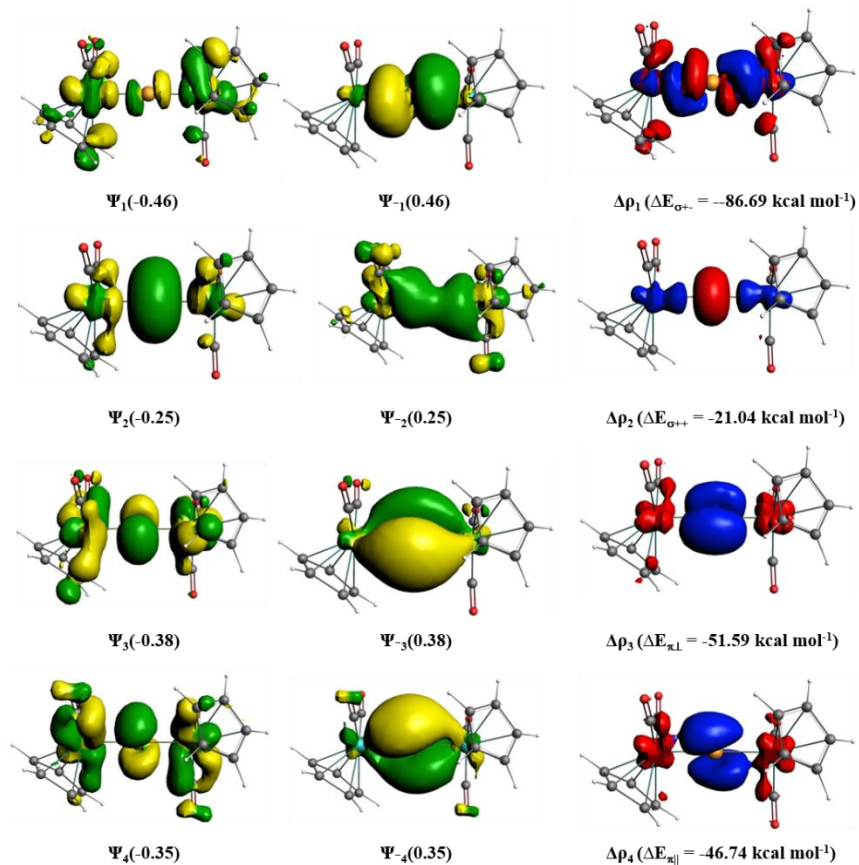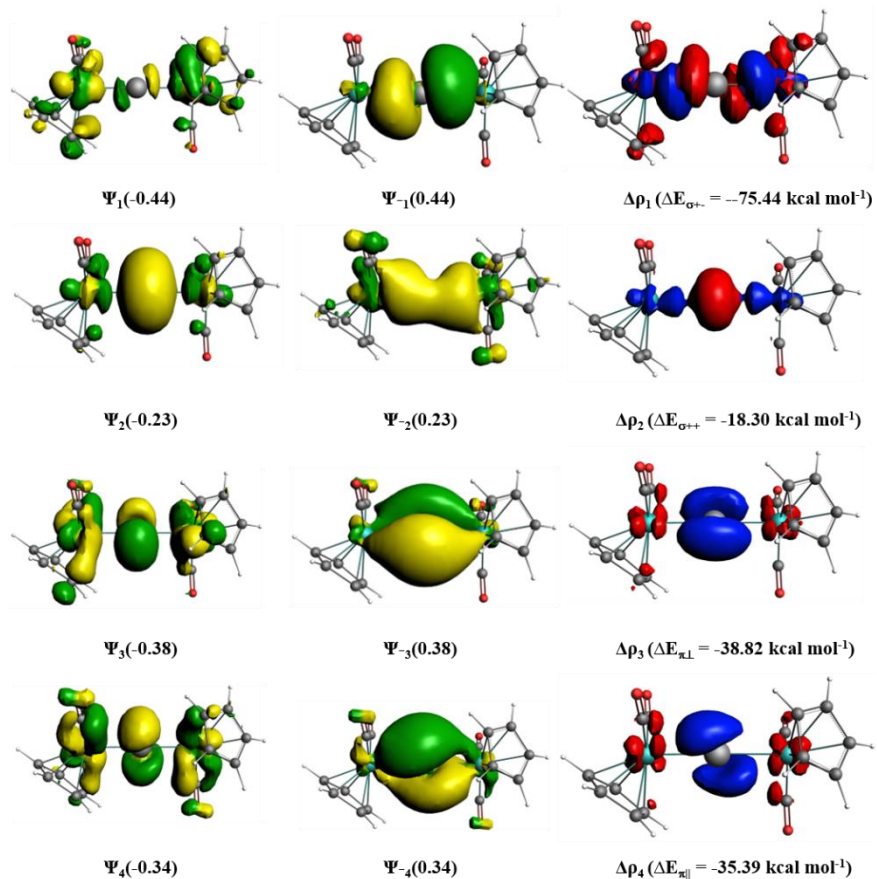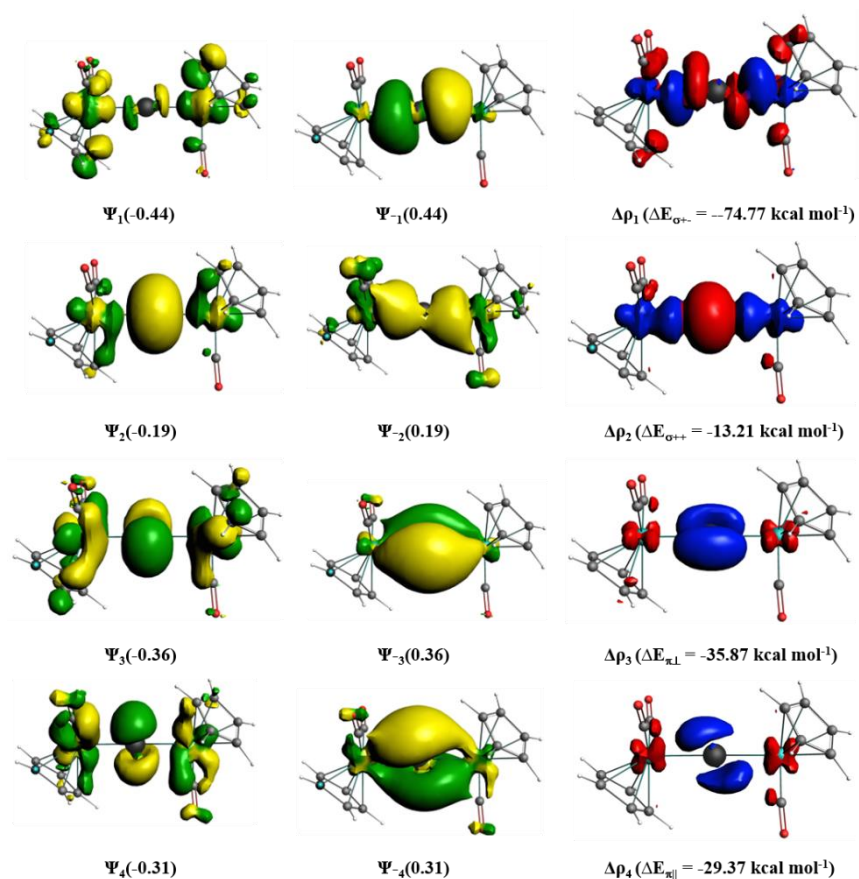
a)

$\Psi_1(-0.44)$ $\Psi_{-1}(0.44)$ $\Delta\rho_1 (\Delta E_{\sigma+-} = -75.44 \text{ kcal mol}^{-1})$

$\Psi_2(-0.23)$ $\Psi_{-2}(0.23)$ $\Delta\rho_2 (\Delta E_{\sigma++} = -18.30 \text{ kcal mol}^{-1})$

$\Psi_3(-0.38)$ $\Psi_{-3}(0.38)$ $\Delta\rho_3 (\Delta E_{\pi\perp} = -38.82 \text{ kcal mol}^{-1})$

$\Psi_4(-0.34)$ $\Psi_{-4}(0.34)$ $\Delta\rho_4 (\Delta E_{\pi\parallel} = -35.39 \text{ kcal mol}^{-1})$

b)

$\Psi_1(-0.44)$ $\Psi_{-1}(0.44)$ $\Delta\rho_1 (\Delta E_{\sigma+-} = -74.77 \text{ kcal mol}^{-1})$

$\Psi_2(-0.19)$ $\Psi_{-2}(0.19)$ $\Delta\rho_2 (\Delta E_{\sigma++} = -13.21 \text{ kcal mol}^{-1})$

$\Psi_3(-0.36)$ $\Psi_{-3}(0.36)$ $\Delta\rho_3 (\Delta E_{\pi\perp} = -35.87 \text{ kcal mol}^{-1})$

$\Psi_4(-0.31)$ $\Psi_{-4}(0.31)$ $\Delta\rho_4 (\Delta E_{\pi\parallel} = -29.37 \text{ kcal mol}^{-1})$

Figure S13: Plots of important alpha-NOCV pair of orbitals Ψ_{-n}/ Ψ_n of bonding possibility C in **2Sn** (a) and **2Pb** (b) with their eigen values in parenthesis, the deformation densities $\Delta\rho_n$ and the corresponding orbital stabilization energies ΔE (kcal mol^{-1}) at the BP86/TZ2P level of theory. The direction of the charge flow in the deformation density plot $\Delta\rho_n$ is from red→blue. The isosurface values for NOCV orbitals and deformation densities are 0.03 and 0.003 respectively
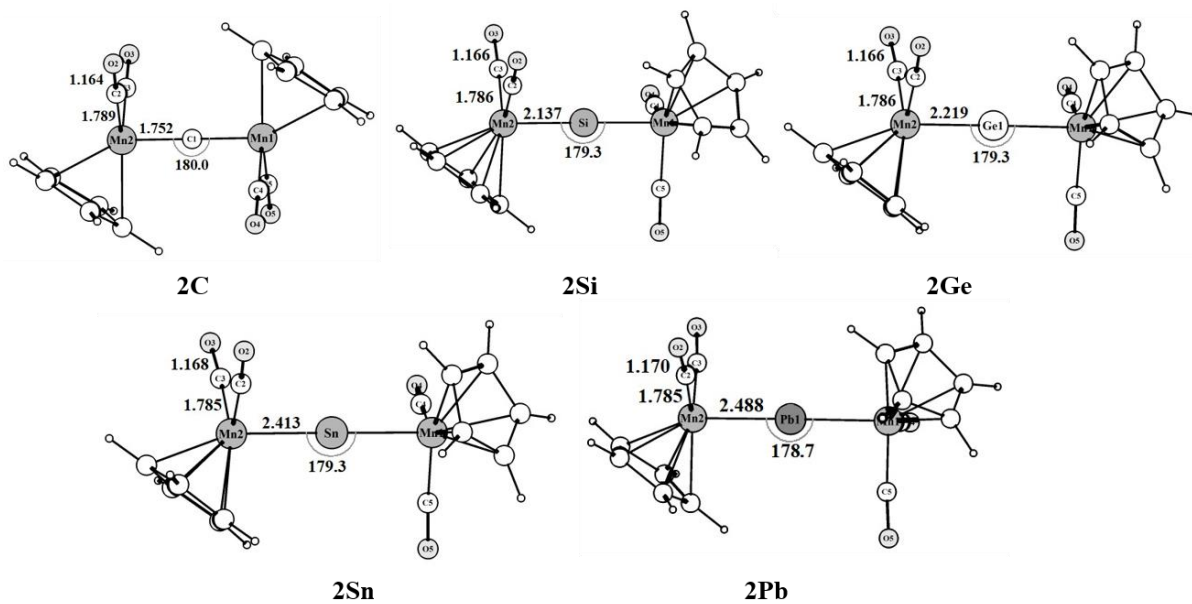
Figure S14: Optimised geometries of 2E (E = C-Pb) at the BP86/def2-TZVPP level of theory.

Table S5: Optimized Cartesian coordinates, total electronic energy E$_{el}$(BP86), zero-point energy, ZPE (BP86) at the BP86/def2-SVP level of theory and the total electronic energy, E$_{el}$ (M06) at the M06/def2-TZVPP level of theory using Gaussian09 program package. The energies are given in a.u

1Si

E$_{el}$(BP86) = -870.6055952 a.u.
ZPE (BP86) = 0.032048 a.u.
E$_{el}$ (M06) = -870.7838461 a.u.

14	0.010947000	-0.508924000	1.291687000
14	0.010947000	1.363292000	0.000000000
1	-0.981295000	-0.593949000	2.427385000
1	0.751414000	-1.824167000	1.249549000
14	0.010947000	-0.508924000	-1.291687000
1	-0.981295000	-0.593949000	-2.427385000
1	0.751414000	-1.824167000	-1.249549000

1Ge

E$_{el}$(BP86) = -6233.404849 a.u.
ZPE (BP86) = 0.028845 a.u.
E$_{el}$ (M06) = -6233.2437827 a.u.

32	0.009045000	-0.593966000	1.400955000
32	0.009045000	1.357172000	0.000000000
1	-1.070989000	-0.688286000	2.531423000
1	0.636824000	-2.019559000	1.267615000
32	0.009045000	-0.593966000	-1.400955000
1	0.636824000	-2.019559000	-1.267615000
1	-1.070989000	-0.688286000	-2.531423000

1Sn

E$_{el}$(BP86) = -645.6417469 a.u.
ZPE (BP86) = 0.024182 a.u.
E$_{el}$ (M06) = -645.5446876 a.u.

50	-0.007677000	-0.711542000	1.621974000
50	-0.007677000	1.551478000	0.000000000
1	1.178905000	-0.873302000	2.901131000
1	-0.603126000	-2.336545000	1.383344000
50	-0.007677000	-0.711542000	-1.621974000
1	-0.603126000	-2.336545000	-1.383344000
1	1.178905000	-0.873302000	-2.901131000

1Pb

E$_{el}$(BP86) = -581.4307656 a.u.
ZPE (BP86) = 0.021553 a.u.
E$_{el}$ (M06) = -581.083086 a.u.

82	0.006681000	-0.751391000	1.752838000
82	0.006681000	1.586836000	0.000000000
1	0.454460000	-2.470467000	1.359059000
1	-1.276251000	-0.975755000	3.033787000
82	0.006681000	-0.751391000	-1.752838000
1	0.454460000	-2.470467000	-1.359059000
1	-1.276251000	-0.975755000	-3.033787000

1Si$_{CH2}$

E$_{el}$(BP86) = -367.9040865 a.u.
ZPE (BP86) = 0.049448 a.u.
E$_{el}$ (M06) = -367. 991526 a.u.

6	0.000000000	0.756122000	-0.783656000
14	0.000000000	0.000000000	0.989692000
1	0.914081000	1.286909000	-1.112954000
1	-0.914081000	1.286909000	-1.112954000
6	0.000000000	-0.756122000	-0.783656000
1	0.914081000	-1.286909000	-1.112954000
1	-0.914081000	-1.286909000	-1.112954000

1Ge$_{CH2}$

E$_{el}$(BP86) = -2155.5076668 a.u.
ZPE (BP86) = 0.049256 a.u.
E$_{el}$ (M06) = -2155.4802745 a.u.

6	0.000000000	0.749390000	-1.237751000
32	0.000000000	0.000000000	0.657432000
1	0.917209000	1.285041000	-1.546203000
1	-0.917209000	1.285041000	-1.546203000
6	0.000000000	-0.749390000	-1.237751000
1	-0.917209000	-1.285041000	-1.546203000
1	0.917209000	-1.285041000	-1.546203000

1Sn$_{CH2}$

E$_{el}$(BP86) = -292.9250352 a.u.
ZPE (BP86) = 0.049000 a.u.
E$_{el}$ (M06) = -292.9181568 a.u.

6	0.000000000	0.740755000	-1.618676000
50	0.000000000	0.000000000	0.541116000
1	-0.920265000	1.279832000	-1.907923000
1	0.920265000	1.279832000	-1.907923000
6	0.000000000	-0.740755000	-1.618676000
1	0.920265000	-1.279832000	-1.907923000
1	-0.920265000	-1.279832000	-1.907923000

1Pb$_{CH2}$

E$_{el}$(BP86) = -271.5299077 a.u.
ZPE (BP86) = 0.049033 a.u.
E$_{el}$ (M06) = -271.4401638 a.u.

6	0.000000000	0.732352000	-1.910029000
82	0.000000000	0.000000000	0.385338000
1	-0.923497000	1.279174000	-2.169351000
1	0.923497000	1.279174000	-2.169351000
6	0.000000000	-0.732352000	-1.910029000
1	-0.923497000	-1.279174000	-2.169351000
1	0.923497000	-1.279174000	-2.169351000

2Si

E$_{el}$(BP86) = -3431.5127257 a.u.
ZPE (BP86) = 0.202501 a.u.
E$_{el}$ (M06) = -3431.6948203 a.u.

14	0.000000000	0.000000000	0.084299000
25	0.000000000	2.128369000	0.029556000
25	0.000000000	-2.128369000	0.029556000
6	-1.639931000	2.068123000	-0.657954000
8	-2.711412000	2.055955000	-1.136378000

6	-0.603657000	2.194955000	1.705227000
8	-0.979689000	2.289746000	2.809827000
6	0.603657000	-2.194955000	1.705227000
8	0.979689000	-2.289746000	2.809827000
6	1.639931000	-2.068123000	-0.657954000
8	2.711412000	-2.055955000	-1.136378000
6	1.103665000	3.969714000	0.248944000
6	0.528916000	3.916445000	-1.057798000
6	1.068465000	2.768078000	-1.737113000
6	1.975486000	2.109046000	-0.839777000
6	2.001821000	2.853437000	0.388573000
1	0.896757000	4.727980000	1.014580000
1	-0.196696000	4.627144000	-1.472950000
1	0.831670000	2.454314000	-2.761305000
1	2.587724000	1.227896000	-1.073360000
6	-1.068465000	-2.768078000	-1.737113000
6	-1.975486000	-2.109046000	-0.839777000
6	-2.001821000	-2.853437000	0.388573000
6	-1.103665000	-3.969714000	0.248944000
6	-0.528916000	-3.916445000	-1.057798000
1	-0.831670000	-2.454314000	-2.761305000
1	-2.587724000	-1.227896000	-1.073360000
1	-2.600967000	-2.614389000	1.275839000
1	-0.896757000	-4.727980000	1.014580000
1	2.600967000	2.614389000	1.275839000
1	0.196696000	-4.627144000	-1.472950000

2Ge

E_{el}(BP86) = -5219.1156771 a.u.
ZPE (BP86) = 0.201475 a.u.
E_{el} (M06) = -5219.1847345 a.u.

32	0.000000000	0.000000000	0.055479000
25	0.000000000	2.206288000	0.022708000
25	0.000000000	-2.206288000	0.022708000
6	-1.717642000	2.211459000	-0.451662000
8	-2.839385000	2.268805000	-0.787959000
6	-0.405390000	2.272764000	1.757190000
8	-0.650052000	2.380843000	2.897053000
6	0.405390000	-2.272764000	1.757190000
8	0.650052000	-2.380843000	2.897053000
6	1.717642000	-2.211459000	-0.451662000
8	2.839385000	-2.268805000	-0.787959000
6	0.769154000	4.200411000	-0.219857000
6	0.417382000	3.663855000	-1.501227000
6	1.223756000	2.502873000	-1.747754000
6	2.073506000	2.308477000	-0.602388000
6	1.789103000	3.352015000	0.338298000
1	0.340513000	5.093823000	0.249957000
1	-0.335956000	4.076789000	-2.184407000
1	1.209085000	1.886709000	-2.655298000
1	2.834993000	1.526129000	-0.488359000
6	-1.223756000	-2.502873000	-1.747754000
6	-2.073506000	-2.308477000	-0.602388000
6	-1.789103000	-3.352015000	0.338298000
6	-0.769154000	-4.200411000	-0.219857000
6	-0.417382000	-3.663855000	-1.501227000
1	-1.209085000	-1.886709000	-2.655298000
1	-2.834993000	-1.526129000	-0.488359000
1	-2.272807000	-3.485123000	1.314380000
1	-0.340513000	-5.093823000	0.249957000
1	2.272807000	3.485123000	1.314380000

1	0.335956000	-4.076789000	-2.184407000

2Sn

E_{el}(BP86) = -3356.5245022 a.u.
ZPE (BP86) = 0.200860 a.u.
E_{el} (M06) = -3356.6148251 a.u.

50	0.000000000	0.000000000	0.032205000
25	0.000000000	2.404271000	0.016062000
25	0.000000000	-2.404271000	0.016062000
6	-1.736622000	2.421147000	-0.381143000
8	-2.871987000	2.510110000	-0.664045000
6	-0.339219000	2.451105000	1.764706000
8	-0.543969000	2.563428000	2.913378000
6	0.339219000	-2.451105000	1.764706000
8	0.543969000	-2.563428000	2.913378000
6	1.736622000	-2.421147000	-0.381143000
8	2.871987000	-2.510110000	-0.664045000
6	0.679760000	4.412850000	-0.277788000
6	0.348035000	3.829335000	-1.545770000
6	1.205692000	2.701327000	-1.768627000
6	2.069841000	2.574971000	-0.623689000
6	1.740983000	3.626793000	0.292706000
1	0.213752000	5.297921000	0.171692000
1	-0.425322000	4.191486000	-2.235399000
1	1.222201000	2.071522000	-2.666898000
1	2.873525000	1.838673000	-0.495627000
6	-1.205692000	-2.701327000	-1.768627000
6	-2.069841000	-2.574971000	-0.623689000
6	-1.740983000	-3.626793000	0.292706000
6	-0.679760000	-4.412850000	-0.277788000
6	-0.348035000	-3.829335000	-1.545770000
1	-1.222201000	-2.071522000	-2.666898000
1	-2.873525000	-1.838673000	-0.495627000
1	-2.222698000	-3.805537000	1.262529000
1	-0.213752000	-5.297921000	0.171692000
1	2.222698000	3.805537000	1.262529000
1	0.425322000	-4.191486000	-2.235399000

2Pb

E_{el}(BP86) = -3335.1232101 a.u.
ZPE (BP86) = 0.200400 a.u.
E_{el} (M06) = -3335.1311544 a.u.

82	0.000000000	0.000000000	0.030478000
25	0.000000000	2.482555000	0.007005000
25	0.000000000	-2.482555000	0.007005000
6	-1.581209000	2.497092000	-0.814031000
8	-2.609852000	2.594396000	-1.371664000
6	-0.756089000	2.548803000	1.618382000
8	-1.236365000	2.681529000	2.680472000
6	0.756089000	-2.548803000	1.618382000
8	1.236365000	-2.681529000	2.680472000
6	1.581209000	-2.497092000	-0.814031000
8	2.609852000	-2.594396000	-1.371664000
6	0.914920000	4.400711000	0.229417000
6	0.600896000	4.179080000	-1.148437000
6	1.345777000	3.036361000	-1.605676000
6	2.115362000	2.545656000	-0.496122000
6	1.854844000	3.386286000	0.635612000
1	0.519012000	5.204733000	0.862016000

1	-0.082532000	4.784771000	-1.757092000
1	1.339411000	2.626635000	-2.623213000
1	2.830522000	1.712883000	-0.525872000
6	-2.115362000	-2.545656000	-0.496122000
6	-1.854844000	-3.386286000	0.635612000
6	-0.914920000	-4.400711000	0.229417000
6	-0.600896000	-4.179080000	-1.148437000
6	-1.345777000	-3.036361000	-1.605676000
1	-2.830522000	-1.712883000	-0.525872000
1	-2.296821000	-3.279041000	1.634089000
1	-0.519012000	-5.204733000	0.862016000
1	0.082532000	-4.784771000	-1.757092000
1	2.296821000	3.279041000	1.634089000
1	-1.339411000	-2.626635000	-2.623213000